

**Integrated analyses of the genetic and clinicopathological features of
cholangiolocarcinoma: cholangiolocarcinoma may be characterized by mismatch-repair
deficiency.**

Kenta Makino¹, Takamichi Ishii^{1*}, Haruhiko Takeda², Yoichi Saito³, Yukio Fujiwara⁴, Masakazu Fujimoto⁵, Takashi Ito¹, Satoshi Wakama¹, Ken Kumagai², Fumiaki Munekage¹, Hiroshi Horie¹, Katsuhiro Tomofuji¹, Yu Oshima¹, Elena Yukie Uebayashi¹, Takayuki Kawai^{1,6}, Satoshi Ogiso¹, Ken Fukumitsu¹, Atsushi Takai², Hiroshi Seno², Etsuro Hatano¹

¹Department of Surgery, Graduate School of Medicine, Kyoto University, Kyoto, Japan

²Department of Gastroenterology and Hepatology, Graduate School of Medicine, Kyoto University, Kyoto, Japan

³Laboratory of Bioengineering, Faculty of Advanced Science and Technology, Kumamoto University, Kumamoto, Japan

⁴Department of Cell Pathology, Graduate School of Medical Sciences, Faculty of Life Sciences, Kumamoto University, Kumamoto, Japan

⁵Department of Diagnostic Pathology, Graduate School of Medicine, Kyoto University, Kyoto, Japan

⁶Department of Surgery, Medical Research Institute Kitano Hospital, Osaka, Japan

***Correspondence to:** T Ishii, Department of Surgery, Graduate School of Medicine, Kyoto University, 54 Kawahara-cho Shogoin, Sakyo-ku, Kyoto, 606-8507, Japan. E-mail:

taishii@kuhp.kyoto-u.ac.jp

Running title: The genetic and clinicopathological features of cholangiocarcinoma

No conflicts of interests were declared

Word count: 3999

Ethics Approval and Consent to Participate:

The study protocol was approved by the Ethics Committee of the Graduate School of Medicine, Kyoto University (R1737-3). This study was conducted in accordance with the principles of the Declaration of Helsinki.

Abstract

Cholangiolocarcinoma (CLC) is a primary liver carcinoma that resembles the canals of Hering and which has been reported to be associated with stem cell features. Due to its rarity, the nature of CLC remains unclear, and its pathological classification remains controversial. To clarify the positioning of CLC in primary liver cancers and identify characteristics that could distinguish CLC from other liver cancers, we performed integrated analyses using whole-exome sequencing (WES), immunohistochemistry, and a retrospective review of clinical information on eight CLC cases and two cases of recurrent CLC. WES demonstrated that CLC includes *IDH1* and *BAP1* mutations, which are characteristic of intrahepatic cholangiocarcinoma (iCCA). A mutational signature analysis showed a pattern similar to that of iCCA, which was different from that of hepatocellular carcinoma (HCC). CLC cells, including CK7, CK19, and EpCAM, were positive for cholangiocytic differentiation markers. However, the hepatocytic differentiation marker AFP and stem cell marker SALL4 were completely negative. The immunostaining patterns of CLC with CD56 and EMA were similar to those of the noncancerous bile ductules. In contrast, mutational signature cluster analyses revealed that CLC formed a cluster associated with mismatch-repair deficiency (dMMR), which was separate from iCCA. Therefore, to evaluate MMR status, we performed immunostaining of four MMR proteins (PMS2, MSH6, MLH1, and MSH2) and detected dMMR in almost all CLCs. In conclusion, CLC had highly similar characteristics to iCCA but not to HCC. CLC can be categorized as a subtype of iCCA. In

contrast, CLC has characteristics of dMMR tumors that are not found in iCCA, suggesting that it should be treated distinctly from iCCA.

Key words:

Cholangiolocarcinoma; Cholangiolocellular carcinoma; Intrahepatic cholangiocarcinoma;

Mismatch-repair deficiency; Whole-exome sequencing; Genetic landscape; Gene mutation;

Liver cancer

Introduction

Cholangiolocarcinoma (CLC), previously known as cholangiolocellular carcinoma, is a rare primary liver carcinoma. Although the cellular origin of CLC is still unclear, it has been suggested to be derived from bile ductules or the canals of Hering [1,2]. Because bipotent hepatic stem or progenitor cells (HpSCs) are thought to exist in these locations, CLC are thought to have differentiation traits for both hepatocellular carcinoma (HCC) and cholangiocarcinoma [3,4]. Accordingly, the World Health Organization (WHO) Classification 2010 classified CLC as a subtype of combined hepatocellular-cholangiocarcinoma (cHCC-CCA) with stem cell features [5]. Subsequently, several studies described CLC as a distinct biliary-derived entity [6,7]. Other studies have suggested that it should be classified as a subtype of small duct-type intrahepatic cholangiocarcinoma (iCCA) based on immunohistochemical similarities and the presence of recurrent genomic aberrations in iCCA, such as *IDH1* mutations [8-10]. According to the WHO classification 2019, CLC without components of HCC or intermediate carcinoma is classified as iCCA [11]. Conversely, the Japanese General Rules for the Clinical and Pathological Study of Primary Liver Cancer classifies CLC as distinct tumors [12]. Therefore, the pathological classification of CLC remains to be established and is controversial.

This rarity hinders the understanding of CLC [3], and a definitive diagnosis is difficult without a pathological evaluation after surgical resection, which further limits the accumulation of cases. Therefore, few genetic analyses have been conducted using next-generation sequencing.

Actually, several genetic alterations have been reported to be associated with CLC, including *IDH1*, *FGFR2*, and *TP53* mutations [6,9,13]. *IDH1* mutations have been widely reported [6,9,13]; however, they are not shared by most CLCs and are not CLC-specific. Previous studies on pure CLC with a high tumor purity have included only a small number of cases and have focused only on hot spots or limited gene mutations [9,13,14], without comprehensive genetic analyses; thus, they do not provide a clear picture of CLC. Additionally, although various international genome projects have been conducted, such as the International Cancer Genome Consortium (ICGC) or The Cancer Genome Atlas (TCGA), they do not include any data on CLC. The absence of public data also hinders the elucidation of CLC.

We aimed to clarify the positioning of CLC in primary liver cancers and identify characteristics that could distinguish CLC from other liver cancers through integrated analyses using whole-exome sequencing, immunohistochemistry, and a retrospective review of clinical information.

Materials and methods

Patients

We enrolled 144 patients with CLC (n=8), iCCA (n=119), or cHCC-CCA (n=17) who underwent surgical resection at Kyoto University from 2005 to 2018. The pathological diagnosis was based on hematoxylin and eosin staining, according to the latest WHO 2019 criteria [11]. The diagnosis of CLC was confirmed by two expert pathologists (MF and YS). The CLC component

was defined based on the extent of nuclear atypia and the architectural growth pattern. Low-grade nuclear atypia and a branching cord-like anastomosing pattern (“antler-like” pattern) resembling a ductular reaction embedded in a fibrous stroma were considered the defining features of CLC [9,11,12,15] (supplementary material, Figure S1). If the CLC component comprised at least 80% of the tumor without hepatocellular differentiation, it was designated as CLC. For whole-exome sequencing of CLC, cancer components were obtained from formalin-fixed paraffin-embedded (FFPE) tissue specimens collected from eight patients with CLC. Recurrent lesions were also obtained from two patients, one involving the CLC inside the liver and the other involving the CCA in the gastric lymph node. Details for DNA extraction are presented in Supplementary materials and methods.

Immunohistochemistry

Immunohistochemical staining was performed on 4- μ m-thick FFPE whole-tissue sections from eight patients with CLC. For comparisons with CLC, whole tissue sections from two patients with small duct-type iCCA, two patients with well-differentiated HCC, and two liver transplant donors (as normal livers) who underwent surgery at Kyoto University were also immunostained. We immunostained for CK7, CK19, AFP, EpCAM, CD56, EMA, SALL4, CD8, PD-L1, and four mismatch repair (MMR) proteins (PMS2, MSH6, MLH1, and MSH2). All immunoreactivities were reviewed and evaluated by pathologists who were blinded to sample

information. A negative expression of MMR proteins was defined as the definite absence of nuclear staining in at least 10% of tumor cells, despite positive staining in the surrounding stromal cells and lymphocytes. Mismatch repair deficiency (dMMR) was defined as the negative expression of at least one MMR protein in tumor cells. Mismatch-repair proficient (pMMR) was defined as the positive expression of all four MMR proteins in all tumor cells [16]. The extent of CD8⁺ T-cell infiltration into the tumor was evaluated using four independent fields at mid-magnification ($\times 10$ magnification objective lens). For EMA, cytoplasmic and membranous staining patterns were recorded for each tumor. Details of the antibodies and dilutions used are summarized in supplementary material, Table S1.

Whole-exome sequencing (WES) of CLCs

Genomic DNA was extracted from each CLC component and recurrent tumor and was subjected to genetic analyses. Exome capture was performed using SureSelect Human All Exon V6 (Agilent Technologies, Santa Clara, CA, USA), according to the manufacturer's instructions. WES was performed using the NovaSeq 6000 platform (Illumina, San Diego, CA, USA) and a 150-bp paired-end read protocol. Sequencing reads were first aligned to NCBI Human Reference Genome Build 38 (hg38) (<https://gdc.cancer.gov/about-data/gdc-data-processing/gdc-reference-files>), and the sequencing data were analyzed for somatic mutation calling using the Genomon2 pipeline (v.2.6) (<https://genomon.readthedocs.io/ja/latest/>), as previously described

[17,18]. Somatic mutations were identified by comparing the tumor and non-tumor liver tissue genomes.

Analysis of mutational signatures

The number of single nucleotide variants (SNVs) assigned to each of the 96 possible substitution classifications, defined by the substitution class and sequence context immediately 5' and 3' to each mutated base in the coding regions, was counted for each sample. The frequency of each mutation was calculated by dividing the count by the total number of mutations. The analysis was conducted using R v.4.1.2 (The R Foundation for Statistical Computing, Vienna, Austria), with the MutationalPatterns package (v.3.4.0) at the default setting [19,20] and based on Mutational Signatures version 3 in the Catalogue of Somatic Mutations in Cancer (COSMIC) (<https://cancer.sanger.ac.uk/signatures>).

Statistical analyses

Statistical analyses were performed using R v.4.1.2 (The R Foundation for Statistical Computing). Continuous data were expressed as the median and range and analyzed using the Kruskal–Wallis test, followed by a pairwise Wilcoxon *post hoc* analysis for comparisons of the three groups. Categorical data among the three groups were analyzed using the chi-squared test followed by Bonferroni adjusted *post hoc* analysis. Survival curves were

estimated using the Kaplan–Meier method and compared using a log-rank test. Statistical significance was set at $P < 0.05$.

The methods used for DNA extraction, mutation calling, Sanger sequencing of *TERT* promoter mutations, microsatellite instability (MSI) evaluation, copy number variation analysis, and reanalysis of public database records are described in Supplementary materials and methods.

Results

Clinicopathological features of CLC

From 2005 to 2018, 1,035 cases underwent hepatectomy for primary liver tumors. The frequency of CLC was 0.77%. The clinicopathological features of CLC, iCCA, and cHCC-CCA are summarized in Table 1 and supplementary material, Table S2. There are some reports of CLC arising in patients with chronic liver diseases [4,21,22], but in this study, none of the CLC cases had underlying cirrhosis and all were negative for hepatitis B surface antigen (HBsAg) and hepatitis C virus antibody (HCV-Ab). Most of the background livers in CLC cases showed no fibrosis. Only two cases showed mild-moderate fibrosis (METAVIR F1 and F2). The underlying hepatic disease was cryptogenic in one case and caused by alcohol use in the other case. These results indicated that CLC is not always associated with chronic hepatitis. Although the clinicopathological features of CLC and the other two tumors were broadly similar, CLC

cases tended to show favorable prognoses. Although the difference was not statistically significant, the CLC cases tended to show less invasion of the major portal vein, hepatic vein, and biliary tract and tended to have a better overall survival (OS) than the other groups (supplementary material, Figure S2). The 5-year OS rates of CLC, iCCA, and cHCC-CCA cases were 75.0%, 39.9%, and 41.5%, respectively. The two patients with CLC who underwent resection for recurrent disease also showed a long-term survival, indicating that surgical resection of recurrent CLC may contribute to a better prognosis. Similar to other tumors, CLC recurred in the remnant liver, lymph nodes, and bones (supplementary material, Table S3). Among them, Case 2 recurred as a CLC inside the remnant liver (Case 2rec), but interestingly, Case 3 recurred as a CCA in the gastric lymph nodes (Case 3rec). Therefore, we included these two recurrent tumors in the subsequent analysis.

CLC cells showed a cholangiocytic immunostaining pattern

To investigate whether CLC cells have bipotentiality, we immunostained for cholangiocytic and hepatocytic differentiation markers and stem cell markers. CLC cells, including CK7, CK19 and EpCAM [15,23,24]. Conversely, they were negative for both the hepatocytic differentiation marker AFP and the stem cell marker SALL4 [25] (Figure1). These staining results were consistent with those of the small duct-type iCCAs. As EMA and CD56 have been reported to show different immunostaining patterns based on the size of the bile ducts [4,26,27], we

compared non-tumor bile ducts and CLC cells. In the non-tumor area, EMA positivity was observed in the cytoplasm of the interlobular bile ducts (Figure 2A) and in the membranes of the ductules in ductular reactions (Figure 2C). The interlobular bile ducts were negative for CD56 (Figure 2B), whereas the proliferated bile ductules were positive for CD56 (Figure 2D). CLC cells showed a similar staining pattern to the ductules in ductular reactions: part of the cells showed membranous positivity for EMA (Figure 2E), and some of the cells were positive for CD56 (Figure 2F). These results suggest that CLC might have the characteristics of bile ducts, especially ductules, rather than HpSCs or hepatocytes.

CLC had iCCA-like driver gene mutations

As the clinical and immunostaining pictures of CLC were similar to those of iCCA, we explored the characteristic gene mutations of CLC through comprehensive genetic analyses. The landscape of genomic aberrations detected by WES is shown in Figure 3. The mean sequence depth for CLCs and their recurrent tumors was 192.1 (supplementary material, Table S4). WES identified 1,322 somatic mutations (881 non-silent and 441 silent) (supplementary material, Table S5). SNVs accounted for most of the mutations (1,129 mutations), followed by INDELS (163 mutations). We could not detect any driver gene mutations shared by any of the CLCs. However, among the detected cancer-related alterations, CLC includes various recurrent mutations in biliary tract cancers (BTC), including *ARID1A*, *ARID1B*, *ARID2*, *BAP1*, *CDKN2A*,

GNAS, *KRAS*, and *IDH1* mutations [28,29]. Typical drivers of iCCA, *IDH1* and *BAP1* alterations have been detected [28-30]. Despite the lack of *FGFR2* fusion, *IDH1* mutations, which are typically detected in small duct-type iCCA [2,31], were detected in two cases. However, CLC does not possess *TERT* promoter mutations, which are the most prevalent genetic alterations in HCC [32-35], or *CTNNB1* and *AXIN1* mutations, which are representative of Wnt/ β -catenin pathway mutations [34,36,37]. CLC also lacks *TP53* mutations, which are repeatedly observed in cHCC-CCA [38-40]. These findings indicate that driver gene mutations for CLC are characteristic mutations of iCCA, but not HCC or cHCC-CCA. Additionally, CLC exhibits several actionable alterations, including *ATM*, *CDKN2A*, *HRAS*, *KRAS*, *IDH1* [30,41].

CLC exhibited a characteristic mutational signature associated with dMMR

Immunohistochemistry and somatic mutations in CLC showed cholangiocytic traits. Recent studies have reported that mutational signature analyses provide clues regarding the process of mutation generation [42,43]. We compared the mutational signatures of CLC with those of iCCA and HCC. Hepatitis B and C were not present in any of the CLC cases. Accordingly, we extracted the whole-genome sequencing data of 7 iCCA Japanese non-BC hepatitis patients and 14 HCC Japanese non-BC hepatitis patients from the ICGC database and compared the point mutations with the primary CLC data. We found that somatic mutations in CLCs were characterized by a predominance of C>T mutations, especially those within the CpG context,

followed by T>C and C>A mutations (Figure 4A). These mutational signatures were similar to those observed in iCCA but differed from those observed in HCC, which predominantly showed T>C mutations. Additionally, we generated 96 trinucleotide mutational signatures and examined their similarity to COSMIC single-base substitution (SBS) signatures (Figure 4B,C). Among the COSMIC signatures to which CLCs showed similarity, SBS1 is a common mutational pattern associated with adenocarcinoma [44]. While these findings also supported the similarity between CLC and iCCA, CLCs formed their own clusters, with the exception of a few iCCAs. To explore different characteristics from iCCA, we further extracted three *de novo* signatures using a non-negative matrix factorization (NMF) analysis [19,20] (supplementary material, Figure S3), and evaluated the relative contributions of each signature for each sample (Figure 4D). The analysis found that almost all CLCs formed SBS6-like characteristic clusters, suggesting that they acquired a dMMR [44,45]. The SBS40-like and SBS12-like clusters formed by iCCA and HCC, respectively, are consistent with previous reports, which suggests the reliability of the cluster analysis results [44].

Almost all CLCs lacked the expression of MMR proteins

A mutational signature analysis suggested that CLCs were associated with dMMR. However, no major alterations in MMR genes were detected in exon regions (supplementary material, Tables S5 and S6). Therefore, we immunostained for four MMR proteins (PMS2, MSH6, MLH1, and

MSH2) [16]. These proteins are not immunostained if the MMR genes are mutated or inactivated. To select these antibodies, we compared the immunostaining of PMS2 and MSH6 using two different antibodies, as they are sufficient for dMMR screening [46,47]. Since the DAKO antibodies stained strongly, and effectively immunostained the pMMR iCCAs as well as the colorectal cancer we previously reported [47] (supplementary material, Table S7), we assessed the immunoreactivity of the four MMR proteins using the DAKO antibodies. As positive controls, we immunostained whole tissue sections from two patients with small duct-type iCCA, two patients with well-differentiated HCC, and two normal livers from transplant donors. All cells were clearly stained and determined to be pMMR (supplementary material, Figure S4). Conversely, almost all CLCs and their recurrent tumors showed dMMR (Figure 3, Figure 5, and supplementary material, Figure S5 and Table S8). However, they showed a range of immunostaining profiles (Figure 5 and supplementary material, Figure S6 and Table S8). Supplementary material, Figure S6 shows the immunostaining profile for PMS2. When we extracted three different regions from one specimen, the tumor cells of small duct-type iCCA were diffusely stained in every region (supplementary material, Figure S6A–C), whereas CLC showed a diffusely positive region (supplementary material, Figure S6D), which is a heterogeneously negative region (supplementary material, Figure S6E) and a completely negative region (supplementary material, Figure S6F). Since these results were shared by other MMR proteins, we defined the negative expression of MMR proteins as the definite absence of

nuclear staining in at least 10% of tumor cells. According to this determination, only case 2 had pMMR and all of the remaining cases had dMMR (Figure 3, Figure 5, and supplementary material, Figure S5 and Table S8). Several CLCs also showed high CD8⁺ tumor infiltrating T cells (TILs) (Figure 3 and Figure 5). In short, CLC had dMMR tumor characteristics that were not found in iCCA.

dMMR and other tumor immune biomarkers in CLCs

dMMR tumors are often associated with tumor immune biomarkers of high tumor mutational burden (TMB-H), microsatellite instability-high (MSI-H) status, and the expression of PD-L1 [16,48]. Therefore, we evaluated the expression of these biomarkers (supplementary material, Table S9). The median TMB of typical iCCA has been reported to be 2.0 [49], and pMMR Case 2 exhibited a similar TMB. Of the eight dMMR CLC tumors, five showed a TMB higher than the median value. Three of the tumors exhibited an MSI-H status and three tumors expressed PD-L1 with a combined positive score (CPS) of >1.

CLC showed heterogeneous copy number variations

We performed whole-exome copy number variation (CNV) analysis of primary CLCs. CLCs presented various CNV patterns in each case, with no common arm-level CNVs (supplementary material, Figures S7A and Figure S8). Owing to the low number of cases, we combined the data

and analyzed them using the GISTIC2. A GISTIC2 analysis demonstrated several amplifications and deletions, but among these regions, we could not detect any important cancer-related genes in BTC or HCC (supplementary material, Figure S7B). These findings indicated that specific CNVs may not be relevant to the tumorigenesis of CLC.

The phylogenetic analysis of somatic mutations supported a genetic association between CLC and CCA.

To examine the evolutionary relationships between primary CLC and recurrent tumors, we constructed a schematic evolutionary tree for cases 2 and 3 based on somatic mutations and estimated the subclonal cellular populations (Figure 6). This analysis was performed using all somatic mutations detectable by WES, including those in non-exonic regions, because SureSelect Human All Exon V6 can also capture considerable non-exonic regions, and evolutionary traits are generally analyzed with the inclusion of passenger mutations (supplementary material, Table S10). In Case 2, which recurred as CLC, the primary tumor cells were partially positive for CD56, and EMA showed heterogeneity of cytoplasmic and membranous positive cells. Recurrent tumor cells preserved this immunostaining profile (Figure 6A). Genetically, primary and recurrent tumors share several common mutations. A phylogenetic analysis suggested that some clones of the primary tumor acquired dMMR, MSI-H status, and TMB-H, and progressed by acquiring driver gene mutations, such as *ARID1A/1B*.

Conversely, in case 3, which recurred as CCA, the immunostaining profiles of the primary and recurrent tumors were different. While the primary tumor included CD56-positive cells, and both the cytoplasm and the membrane of the cells were positive for EMA, the recurrent tumors lacked CD56-positive cells and cells with membranous positivity for EMA, which is a characteristic of the bile ductules. Furthermore, the genomic profiles of primary and recurrent tumors were different. Only in the primary tumor, *IDH1* frameshift was detected as a driver gene mutation, and we found clusters of point mutations, so-called kataegis events on chromosome 19. Notably, however, the primary tumor and the recurrent tumor shared a few common mutations (Figure 6B), suggesting that the two tumors originated from the same cell population but evolved separately at an early stage of carcinogenesis and supported a genetic association between CLC and CCA.

Discussion

More than 60 years have passed since Steiner and Higginson first reported CLC in 1959 [1]. However, their nature remains unclear. CLC are considered to be derived from the canals of Hering owing to their pathological morphology [1,2]. Since the canals of Hering are thought to contain HpSCs, CLC have been thought to be associated with stem cell features [3,4]. Although recent developments in next generation sequencing techniques have revealed genomic aberrations in CLC [6,9,13,14], previous reports included only a small number of cases and

analyzed limited genetic mutations; thus, the specific characteristics of CLC remain unknown. Among the studies in the literature, our study, which included comprehensive genetic analyses, analyzed the largest number of strictly defined CLC cases. This study combined WES, immunohistopathology, and retrospective review of clinical information to provide a more detailed picture of the nature of CLC.

In the WES data of this study, CLC was found to have somatic mutations characteristic of iCCA. Previous reports have suggested that CLC is a subtype of iCCA because it expresses a biliary molecular profile [6] and exhibits somatic mutations characteristic of iCCA, including *IDH1/2* and *FGFR2* mutations [9]. We herein found multiple somatic mutations that are commonly observed in BTC [28,29], as well as *IDH1* and *BAP1* mutations, which are characteristic of iCCA [28-30]. In particular, *IDH1*, which is a known driver gene for small duct-type iCCA [2,31], was mutated in several CLC cases in this study. A mutational signature analysis showed a similar pattern to that of iCCA, namely, a predominance of C>T mutations, especially those within the CpG context, followed by T>C and C>A mutations. In contrast, *TERT* promoter mutations, which are the most prevalent genetic alterations in HCC [32-35], were not found in CLC, and a mutational signature analysis showed a different pattern between CLC and HCC. The finding that CLC showed similarity to SBS1, which is a mutational pattern frequently associated with adenocarcinomas [44], supported the observation that CLC was similar to iCCA, but not HCC. Furthermore, we analyzed a case of lymph node recurrence of

CCA after hepatic resection for CLC. A phylogenetic tree analysis showed that the primary and recurrent CCA tumors shared common mutations, suggesting that the primary CLC tumor and recurrent CCA tumor originated from the same cell population and supported a genetic association between CLC and CCA. Additionally, immunostaining of CLC showed the same staining patterns as those of CD56 and EMA, as previously reported for CLC [4,6,21,26,27,50]. We further compared the staining patterns of CLC with CD56 and EMA with those of the interlobular bile ducts and bile ductules in normal liver tissue and revealed that some of the CLC cells showed similar staining patterns to those of bile ductules. The stem cell marker SALL4 [25] and hepatocytic differentiation marker were negative for CLC. Considering the above findings, CLC showed similarity to iCCA, particularly to much smaller iCCA, while CLC cells may not have bipotentiality.

Although the clinical, immunohistochemical, and genetic features of CLC are very similar to those of iCCA, mutational signature cluster analyses revealed that CLC formed a separate cluster from most iCCAs. Additionally, CLC had a lower tendency to invade the bile ducts or vessels and tended to show a better prognosis than iCCA. These findings suggest that CLC has different characteristics than iCCA, which might be significant for distinguishing CLC from iCCA.

The findings in this study showed that the mutational signature of CLC was analogous to SBS 6 and 15, which are dMMR-related signatures, and that the *de novo* signature was

similar to that of SBS 6, suggesting that CLC might be characterized by dMMR. Therefore, we evaluated four MMR proteins by immunostaining, which is recommended for the identification of dMMR [16]. The frequency of dMMR/MSI-high in biliary tract cancers has been reported to be 1–2% [30,51-53]. However, almost all CLC cases in this study had a dMMR. The lack of significant changes in copy numbers also supports this result. The MSI status has been reported to be a continuous variable, not a discrete one, even within MSS and MSI-H tumors across various carcinomas [54], which is consistent with the wide range of immunostaining profiles of MMR proteins observed in our study. Furthermore, it has been reported that the heterogeneous loss of MMR protein expression is related to dMMR and is not necessarily an artifact [55].

CLC may be considered an immune-hot tumor. This is because dMMR tumors are more susceptible to T-cell recognition by neoantigens [56,57]. The dMMR, MSI-H, TMB-H, and PD-L1 expression statuses are often not consistent with one another and should be regarded as separate biomarkers; however, they generally show some affinity and are associated with tumor immunity [16,48]. CLC tended to have a higher TMB than iCCA. CLC showed highly heterogeneous immunostaining profiles of MMR genes; therefore, the coexistence of both dMMR and pMMR cells in the extracted DNA may potentially suppress the MSI score, but several CLCs showed an MSI-H status. As previously reported, the PD-L1 expression is infrequently observed in adenocarcinomas other than non-small cell lung cancer [58]. It was evident from the low cutoff value for PD-L1 positivity in the companion diagnosis of PD-1/PD-

L1 inhibitors that the PD-L1 expression was low. However, in the present study, we confirmed its expression in several CLCs. Furthermore, although tumors with mutations in the Wnt/ β pathway are said to be immune cold tumors, CLC does not have mutations in the Wnt/ β -catenin pathway, including *CTNNB1* mutations [37,59,60]. In summary, although the mechanism remains unclear, the characteristics of dMMR might be unique to CLC and immune checkpoint inhibitors could be effective against CLC.

The present study is associated with two limitations. First, CLC has a much greater stromal component, resulting in low tumor purity. Therefore, the sensitivity of WES is not high enough to detect low-abundance subclonal gene mutations. However, this means that significant gene mutations relevant to CLC were detected in the current study. Second, owing to the low number of cases, the statistical analysis was insufficient, and the data presented in this study may not be fully generalizable [61]. Therefore, future large-scale studies are warranted.

In conclusion, CLC had characteristics that were closely similar to iCCA, especially to small duct-type iCCA, but not to HCC. On the other hand, by combining the genetic, immunohistochemical, and clinical features, we characterized CLC for the first time. CLC has dMMR tumor characteristics that are not found in iCCA. We hypothesized that treatment with immune checkpoint inhibitors would be beneficial for CLC. The results of the present study suggest that CLC should be treated as a disease that is distinct from iCCA.

Acknowledgements

The authors thank the Center for Anatomical, Pathological and Forensic Medical Research, Kyoto University Graduate School of Medicine, for preparing microscope slides. Nakamura H. and Motoyoshi T. (K.I. Stainer Inc., Kumamoto, Japan) provided excellent histological analyses. This work was supported by JSPS KAKENHI Grant Number 19K09145, 19K07459, 22K04845 and 23K06362.

Author contributions statement

K.M., T.I.¹ and H.T. performed the study concept and design. K.M., T.I.² and S.W. acquired the data. K.M., H.T., Y.S., Y.F., M.F., T.I.², S.W. and K.K. analyzed and interpreted the data. K.M. and T.I.¹ drafted the manuscript. T.I.¹, H.T., Y.S. and Y.F. critically revised the manuscript for important intellectual content. K.M. and T.I.² carried out statistical analysis. F.M., H.H., K.T., Y.O., E.U., T.K., S.O, K.F, A.T. and H.S. provided administrative, technical, or material support. T.I.¹, and E.H. supervised the study. All authors have read and approved the final manuscript.

Data availability statement

The sequence data have been deposited in the Japanese Genotype– phenotype Archive (<https://trace.ddbj.nig.ac.jp/jga>), which is hosted by DDBJ under accession number JGAS000597. (<https://humandbs.biosciencedbc.jp/en/hum0385-v1>).

References

1. Steiner PE, Higginson J. Cholangiolocellular carcinoma of the liver. *Cancer* 1959; **12**: 753-759.
2. Banales JM, Marin JJG, Lamarca A, *et al.* Cholangiocarcinoma 2020: the next horizon in mechanisms and management. *Nat Rev Gastroenterol Hepatol* 2020; **17**: 557-588.
3. Shiota K, Taguchi J, Nakashima O, *et al.* Clinicopathologic study on cholangiolocellular carcinoma. *Oncol Rep* 2001; **8**: 263-268.
4. Komuta M, Spee B, Vander Borgh S, *et al.* Clinicopathological study on cholangiolocellular carcinoma suggesting hepatic progenitor cell origin. *Hepatology* 2008; **47**: 1544-1556.
5. Bosman FT, International Agency for Research on C. WHO classification of tumours of the digestive system. (4th ed). Lyon: International Agency for Research on Cancer, 2010.
6. Moeini A, Sia D, Zhang Z, *et al.* Mixed hepatocellular cholangiocarcinoma tumors: Cholangiolocellular carcinoma is a distinct molecular entity. *J Hepatol* 2017; **66**: 952-961.
7. Sasaki M, Sato Y, Nakanuma Y. Cholangiolocellular Carcinoma With "Ductal Plate Malformation" Pattern May Be Characterized by ARID1A Genetic Alterations. *Am J Surg Pathol* 2019; **43**: 352-360.
8. Aishima S, Oda Y. Pathogenesis and classification of intrahepatic cholangiocarcinoma:

- different characters of perihilar large duct type versus peripheral small duct type. *J Hepatobiliary Pancreat Sci* 2015; **22**: 94-100.
9. Balitzer D, Joseph NM, Ferrell L, *et al.* Immunohistochemical and molecular features of cholangiolocellular carcinoma are similar to well-differentiated intrahepatic cholangiocarcinoma. *Mod Pathol* 2019; **32**: 1486-1494.
 10. Chung T, Rhee H, Nahm JH, *et al.* Clinicopathological characteristics of intrahepatic cholangiocarcinoma according to gross morphologic type: cholangiolocellular differentiation traits and inflammation- and proliferation-phenotypes. *HPB (Oxford)* 2020; **22**: 864-873.
 11. Board WHOCoTE, International Agency for Research on C. Digestive system tumours. (5th ed). International Agency for Research on Cancer, 2019.
 12. Japan LCSGo. General Rules for the Clinical and Pathological Study of Primary Liver Cancer. (6th ed). Osaka: Kanehara & Co., 2015.
 13. Kusano H, Naito Y, Mihara Y, *et al.* Distinctive clinicopathological features and KRAS and IDH1/2 mutation status of cholangiolocellular carcinoma. *Hepatol Res* 2020; **50**: 84-91.
 14. Kawai-Kitahata F, Asahina Y, Kaneko S, *et al.* Comprehensive genetic analysis of cholangiolocellular carcinoma with a coexistent hepatocellular carcinoma-like area and metachronous hepatocellular carcinoma. *Hepatol Res* 2019; **49**: 1466-1474.

15. Brunt E, Aishima S, Clavien PA, *et al.* cHCC-CCA: Consensus terminology for primary liver carcinomas with both hepatocytic and cholangiocytic differentiation. *Hepatology* 2018; **68**: 113-126.
16. Luchini C, Bibeau F, Ligtenberg MJL, *et al.* ESMO recommendations on microsatellite instability testing for immunotherapy in cancer, and its relationship with PD-1/PD-L1 expression and tumour mutational burden: a systematic review-based approach. *Ann Oncol* 2019; **30**: 1232-1243.
17. Yokoyama A, Kakiuchi N, Yoshizato T, *et al.* Age-related remodelling of oesophageal epithelia by mutated cancer drivers. *Nature* 2019; **565**: 312-317.
18. Kakiuchi N, Yoshida K, Uchino M, *et al.* Frequent mutations that converge on the NFKBIZ pathway in ulcerative colitis. *Nature* 2020; **577**: 260-265.
19. Blokzijl F, Janssen R, van Boxtel R, *et al.* MutationalPatterns: comprehensive genome-wide analysis of mutational processes. *Genome Med* 2018; **10**: 33.
20. Manders F, Brandsma AM, de Kanter J, *et al.* MutationalPatterns: the one stop shop for the analysis of mutational processes. *BMC Genomics* 2022; **23**: 134.
21. Ariizumi S, Kotera Y, Katagiri S, *et al.* Long-term survival of patients with cholangiolocellular carcinoma after curative hepatectomy. *Ann Surg Oncol* 2014; **21** **Suppl 3**: S451-458.
22. Liao JY, Tsai JH, Yuan RH, *et al.* Morphological subclassification of intrahepatic

- cholangiocarcinoma: etiological, clinicopathological, and molecular features. *Mod Pathol* 2014; **27**: 1163-1173.
23. Torbenson M, Zen Y, Yeh MM. Tumors of the liver. ed). Rockville, MD: American Registry of Pathology, 2018.
 24. Sciarra A, Park YN, Sempoux C. Updates in the diagnosis of combined hepatocellular-cholangiocarcinoma. *Hum Pathol* 2020; **96**: 48-55.
 25. Yong KJ, Gao C, Lim JS, *et al.* Oncofetal gene SALL4 in aggressive hepatocellular carcinoma. *N Engl J Med* 2013; **368**: 2266-2276.
 26. Komuta M, Govaere O, Vandecaveye V, *et al.* Histological diversity in cholangiocellular carcinoma reflects the different cholangiocyte phenotypes. *Hepatology* 2012; **55**: 1876-1888.
 27. Maeno S, Kondo F, Sano K, *et al.* Morphometric and immunohistochemical study of cholangiolocellular carcinoma: comparison with non-neoplastic cholangiole, interlobular duct and septal duct. *J Hepatobiliary Pancreat Sci* 2012; **19**: 289-296.
 28. Nakamura H, Arai Y, Totoki Y, *et al.* Genomic spectra of biliary tract cancer. *Nat Genet* 2015; **47**: 1003-1010.
 29. Jain A, Kwong LN, Javle M. Genomic Profiling of Biliary Tract Cancers and Implications for Clinical Practice. *Curr Treat Options Oncol* 2016; **17**: 58.
 30. Bekaii-Saab TS, Bridgewater J, Normanno N. Practical considerations in screening for

- genetic alterations in cholangiocarcinoma. *Ann Oncol* 2021; **32**: 1111-1126.
31. Kendall T, Verheij J, Gaudio E, *et al.* Anatomical, histomorphological and molecular classification of cholangiocarcinoma. *Liver Int* 2019; **39 Suppl 1**: 7-18.
 32. Nault JC, Mallet M, Pilati C, *et al.* High frequency of telomerase reverse-transcriptase promoter somatic mutations in hepatocellular carcinoma and preneoplastic lesions. *Nat Commun* 2013; **4**: 2218.
 33. Nault JC, Calderaro J, Di Tommaso L, *et al.* Telomerase reverse transcriptase promoter mutation is an early somatic genetic alteration in the transformation of premalignant nodules in hepatocellular carcinoma on cirrhosis. *Hepatology* 2014; **60**: 1983-1992.
 34. Totoki Y, Tatsuno K, Covington KR, *et al.* Trans-ancestry mutational landscape of hepatocellular carcinoma genomes. *Nat Genet* 2014; **46**: 1267-1273.
 35. Takeda H, Takai A, Kumagai K, *et al.* Multiregional whole-genome sequencing of hepatocellular carcinoma with nodule-in-nodule appearance reveals stepwise cancer evolution. *J Pathol* 2020; **252**: 398-410.
 36. Shibata T, Aburatani H. Exploration of liver cancer genomes. *Nat Rev Gastroenterol Hepatol* 2014; **11**: 340-349.
 37. Rebouissou S, Nault JC. Advances in molecular classification and precision oncology in hepatocellular carcinoma. *J Hepatol* 2020; **72**: 215-229.
 38. Cazals-Hatem D, Rebouissou S, Bioulac-Sage P, *et al.* Clinical and molecular analysis of

- combined hepatocellular-cholangiocarcinomas. *J Hepatol* 2004; **41**: 292-298.
39. Liu ZH, Lian BF, Dong QZ, *et al.* Whole-exome mutational and transcriptional landscapes of combined hepatocellular cholangiocarcinoma and intrahepatic cholangiocarcinoma reveal molecular diversity. *Biochim Biophys Acta Mol Basis Dis* 2018; **1864**: 2360-2368.
40. Joseph NM, Tsokos CG, Umetsu SE, *et al.* Genomic profiling of combined hepatocellular-cholangiocarcinoma reveals similar genetics to hepatocellular carcinoma. *J Pathol* 2019; **248**: 164-178.
41. Okawa Y, Ebata N, Kim NKD, *et al.* Actionability evaluation of biliary tract cancer by genome transcriptome analysis and Asian cancer knowledgebase. *Oncotarget* 2021; **12**: 1540-1552.
42. Greenman C, Stephens P, Smith R, *et al.* Patterns of somatic mutation in human cancer genomes. *Nature* 2007; **446**: 153-158.
43. Olivier M, Weninger A, Ardin M, *et al.* Modelling mutational landscapes of human cancers in vitro. *Sci Rep* 2014; **4**: 4482.
44. Alexandrov LB, Kim J, Haradhvala NJ, *et al.* The repertoire of mutational signatures in human cancer. *Nature* 2020; **578**: 94-101.
45. Alexandrov LB, Nik-Zainal S, Wedge DC, *et al.* Signatures of mutational processes in human cancer. *Nature* 2013; **500**: 415-421.

46. Shia J, Tang LH, Vakiani E, *et al.* Immunohistochemistry as first-line screening for detecting colorectal cancer patients at risk for hereditary nonpolyposis colorectal cancer syndrome: a 2-antibody panel may be as predictive as a 4-antibody panel. *Am J Surg Pathol* 2009; **33**: 1639-1645.
47. Saito Y, Fujiwara Y, Miyamoto Y, *et al.* CD169(+) sinus macrophages in regional lymph nodes do not predict mismatch-repair status of patients with colorectal cancer. *Cancer Med* 2023; **12**: 10199-10211.
48. Zang YS, Dai C, Xu X, *et al.* Comprehensive analysis of potential immunotherapy genomic biomarkers in 1000 Chinese patients with cancer. *Cancer Med* 2019; **8**: 4699-4708.
49. Zhang Y, Ma Z, Li C, *et al.* The genomic landscape of cholangiocarcinoma reveals the disruption of post-transcriptional modifiers. *Nat Commun* 2022; **13**: 3061.
50. Nguyen Canh H, Takahashi K, Yamamura M, *et al.* Diversity in cell differentiation, histology, phenotype and vasculature of mass-forming intrahepatic cholangiocarcinomas. *Histopathology* 2021; **79**: 731-750.
51. Le DT, Durham JN, Smith KN, *et al.* Mismatch repair deficiency predicts response of solid tumors to PD-1 blockade. *Science* 2017; **357**: 409-413.
52. Goeppert B, Roessler S, Renner M, *et al.* Mismatch repair deficiency is a rare but putative therapeutically relevant finding in non-liver fluke associated

- cholangiocarcinoma. *Br J Cancer* 2019; **120**: 109-114.
53. Akagi K, Oki E, Taniguchi H, *et al.* Real-world data on microsatellite instability status in various unresectable or metastatic solid tumors. *Cancer Sci* 2021; **112**: 1105-1113.
54. Hause RJ, Pritchard CC, Shendure J, *et al.* Classification and characterization of microsatellite instability across 18 cancer types. *Nat Med* 2016; **22**: 1342-1350.
55. McCarthy AJ, Capo-Chichi JM, Spence T, *et al.* Heterogenous loss of mismatch repair (MMR) protein expression: a challenge for immunohistochemical interpretation and microsatellite instability (MSI) evaluation. *J Pathol Clin Res* 2019; **5**: 115-129.
56. Le DT, Uram JN, Wang H, *et al.* PD-1 Blockade in Tumors with Mismatch-Repair Deficiency. *N Engl J Med* 2015; **372**: 2509-2520.
57. Dudley JC, Lin MT, Le DT, *et al.* Microsatellite Instability as a Biomarker for PD-1 Blockade. *Clin Cancer Res* 2016; **22**: 813-820.
58. Saito Y, Fujiwara Y, Shinchu Y, *et al.* Classification of PD-L1 expression in various cancers and macrophages based on immunohistocytological analysis. *Cancer Sci* 2022; **113**: 3255-3266.
59. Gong J, Chehrazi-Raffle A, Reddi S, *et al.* Development of PD-1 and PD-L1 inhibitors as a form of cancer immunotherapy: a comprehensive review of registration trials and future considerations. *J Immunother Cancer* 2018; **6**: 8.
60. Luke JJ, Bao R, Sweis RF, *et al.* WNT/ β -catenin Pathway Activation Correlates with

- Immune Exclusion across Human Cancers. *Clin Cancer Res* 2019; **25**: 3074-3083.
61. Fujimoto A, Furuta M, Shiraishi Y, *et al.* Whole-genome mutational landscape of liver cancers displaying biliary phenotype reveals hepatitis impact and molecular diversity. *Nat Commun* 2015; **6**: 6120.
 62. Al Bakir M, Huebner A, Martínez-Ruiz C, *et al.* The evolution of non-small cell lung cancer metastases in TRACERx. *Nature* 2023; **616**: 534-542.
 63. Shiraishi Y, Sato Y, Chiba K, *et al.* An empirical Bayesian framework for somatic mutation detection from cancer genome sequencing data. *Nucleic Acids Res* 2013; **41**: e89.
 64. Thorvaldsdóttir H, Robinson JT, Mesirov JP. Integrative Genomics Viewer (IGV): high-performance genomics data visualization and exploration. *Brief Bioinform* 2013; **14**: 178-192.
 65. Wang K, Li M, Hakonarson H. ANNOVAR: functional annotation of genetic variants from high-throughput sequencing data. *Nucleic Acids Res* 2010; **38**: e164.
 66. Tamura K, Stecher G, Kumar S. MEGA11: Molecular Evolutionary Genetics Analysis Version 11. *Mol Biol Evol* 2021; **38**: 3022-3027.
 67. Niu B, Ye K, Zhang Q, *et al.* MSIsensor: microsatellite instability detection using paired tumor-normal sequence data. *Bioinformatics* 2014; **30**: 1015-1016.
 68. Talevich E, Shain AH, Botton T, *et al.* CNVkit: Genome-Wide Copy Number Detection

and Visualization from Targeted DNA Sequencing. *PLoS Comput Biol* 2016; **12**: e1004873.

69. Reich M, Liefeld T, Gould J, *et al.* GenePattern 2.0. *Nat Genet* 2006; **38**: 500-501.

70. Mermel CH, Schumacher SE, Hill B, *et al.* GISTIC2.0 facilitates sensitive and confident localization of the targets of focal somatic copy-number alteration in human cancers. *Genome Biol* 2011; **12**: R41.

References 62–70 are cited only in supplementary material

Figure Legends

Figure 1. Immunostaining profile of CLC, small duct-type iCCA, and well-differentiated HCC.

Representative morphological and immunohistochemical staining features observed in CLC, small duct-type iCCA, and well-differentiated HCC tumor cells. Scale bar, 100 μm .

Figure 2. Immunohistochemical staining for EMA and CD56.

(A–D) Immunohistochemical staining of the bile ducts in the non-tumor area. Scale bar, 50 μm .

(A) Cytoplasmic positivity for EMA was detected in the interlobular bile ducts. (B) The interlobular bile ducts were negative for CD56. (C) Membranous positivity for EMA was detected in the ductules in ductular reaction. (D) CD56 positivity was detected in proliferated bile ductules. (E) Partially membranous positivity for EMA was detected in CLC cells. Scale bar, 50 μm . (F) CLC cells were partially positive for CD56. Scale bar, 100 μm .

Figure 3. Summary of genomic aberrations detected by whole-exome sequencing and MMR status.

Each column represents one sample, and each row represents mutated cancer-related genes, deficient MMR proteins, and the extent of CD8⁺ T cell infiltration into the tumor of each sample. The case number is shown at the top of the figure, and the color key is shown on the

right. Various iCCA-related genes were mutated, whereas CLCs did not possess *TERT* promoter mutations, which are the most prevalent genetic alterations in HCC. With the exception of Case 2, almost all CLCs were dMMR. Several CLCs showed large numbers of CD8⁺ tumor-infiltrating T-cells.

Figure 4. Mutational signatures detected in CLCs, iCCAs, and HCCs.

(A) Mutation patterns determined in CLCs, iCCAs and HCCs. (B) Ninety-six mutational patterns of CLCs, iCCAs and HCCs are shown. Each context is described at the bottom. The Y-axis shows the relative contribution of each context. (C) Cosine similarities between the mutational signatures of each case and COSMIC signature. Each COSMIC signature is described at the bottom. The Y-axis represents each case. (D) Relative contributions of *de novo* mutational signatures in each case. The X-axis demonstrates each *de novo* signature. The Y-axis represents each case. SBS, single-base substitution.

Figure 5. Immunohistochemistry for MMR proteins and CD8⁺ T-cells in CLCs and their recurrent tumors.

All CLC specimens and recurrent tumors are shown. Scale bars for MMR proteins are 50 μ m. Scale bars for CD8 represent 100 μ m.

Figure 6. The phylogenetic analysis of somatic mutations.

Schematic phylogenetic trees based on genetic information (top) and immunohistochemical staining of EMA and CD56 (bottom) of the two cases are shown. In each tree, the trunks are shown in blue, and branches toward primary and recurrent tumors are colored brown and red, respectively. Known biliary cancer-associated driver genes with some genetic aberrations are described in each tree according to the estimated phase at which the aberrations accumulate in tumor cells. Chr, chromosome; TMB, tumor mutation burden.

SUPPLEMENTARY MATERIAL ONLINE

Supplementary materials and methods

Figure S1. Representative histological features of cholangiocarcinoma.

Figure S2. The survival analysis plots for overall survival and recurrence-free survival in CLC, iCCA and cHCC-CCA cases for which surgical resection was performed.

Figure S3. Contribution of the three de novo mutational signatures among the CLCs, iCCAs and HCCs.

Figure S4. Immunohistochemistry for MMR proteins in normal liver tissue, small duct-type iCCA, and well-differentiated HCC.

Figure S5. Immunohistochemistry for MMR proteins.

Figure S6. Immunostaining profiles of PMS2.

Figure S7. Whole-exome copy number variation analyses of primary CLCs.

Figure S8. The landscape of whole-exome copy number variation determined by CNVkit.

Table S1. Details of the antibodies used for immunohistochemistry.

Table S2. The clinical features of cholangiocarcinoma.

Table S3. The sites of recurrence of CLC, iCCA and cHCC-CCA.

Table S4. Mutation profiles of CLCs and their recurrent tumors.

Table S5. Somatic mutations in tumor tissue detected by whole exome sequencing.

Table S6. The sequencing coverages of MMR genes.

Table S7. The comparison of immunostaining intensity between antibodies for PMS2 and MSH6.

Table S8. The proportion of MMR protein-positive cells in tumor cells.

Table S9. TMB, MSI score and PD-L1 score of CLCs and their recurrent tumors.

Table S10. Somatic mutations used for the phylogenetic analysis.

Table 1. The clinicopathological characteristics of the CLC, iCCA, and cHCC-CCA cases.

	CLC (n=8)	iCCA (n=119)	cHCC-CCA (n=17)	P-value	Statistical analysis
Age (years), median (range)	73 (56–83)	69 (32–84)	65 (45–81)	0.216	NS
Sex	Male: 7 Female: 1	Male: 69 Female: 50	Male: 10 Female: 7	0.256	NS
Platelet number ($\times 10^4/\mu\text{l}$), median (range)	208.00 (13.20–281.00)	188.00 (12.90–514.00)	142.00 (32.00–490.00)	0.330	NS
Total bilirubin (mg/dl), median (range)	0.85 (0.60–1.10)	0.70 (0.30–7.20)	1.00 (1.00–4.00)	<0.001	CLC vs. cHCC-CCA: <i>P</i> =0.002 iCCA vs. cHCC-CCA: <i>P</i> <0.001
Albumin (g/dl), median (range)	4.40 (3.40–4.70)	4.00 (2.00–4.90)	4.00 (3.00–5.00)	0.402	NS
Prothrombin time (%), median (range)	88.00 (27.00–122.00)	94.00 (27.00–131.00)	82.00 (65.00–120.00)	0.004	iCCA vs. cHCC-CCA: <i>P</i> =0.003
HBsAg	Positive: 0 Negative: 8 (100%) Missing data: 0	Positive: 5 (4.2%) Negative: 111 (93.3%) Missing data: 3	Positive: 2 (11.8%) Negative: 15 (88.2%) Missing data: 0	0.335	NS
HCV-Ab	Positive: 0 Negative: 8 (100%) Missing data: 0	Positive: 17 (14.3%) Negative: 100 (84.0%) Missing data: 2	Positive: 9 (52.9%) Negative: 8 (47.1%) Missing data: 0	<0.001	iCCA vs. cHCC-CCA: <i>P</i> =0.002

AFP (ng/ml), median (range)	4.80 (1.70–115.20)	3.60 (1.10–160.6)	11.00 (2.00–1517.00)	0.004	iCCA vs. cHCC-CCA: <i>P</i> =0.004
DCP (mAU/ml), median (range)	42.00 (24.00–18851.00)	21.00 (9.00–37836.00)	59.00 (13.00–22480.00)	0.007	CLC vs. iCCA: <i>P</i> =0.011
CEA (ng/ml), median (range)	2.95 (0.90–6.40)	3.10 (0.40–133.10)	3.00 (1.00–13.00)	0.810	NS
CA19-9 (U/ml), median (range)	26.35 (0.60–1467.60)	38.20 (0.00–5461.40)	32.50 (1.00–121.00)	0.537	NS
Tumor number, median (range)	1.00 (1.00–4.00)	1.00 (1.00–5.00)	1.00 (1.00–2.00)	0.870	NS
Tumor size (cm), median (range)	4.00 (1.20–15.00)	4.00 (1.00–20.00)	4.00 (1.00–13.00)	0.993	NS
Major portal vein invasion	Presence: 1 (12.5%)	Presence: 56 (47.1%)	Presence: 7 (41.2%)	0.157	NS
Major hepatic vein invasion	Presence: 0	Presence: 25 (21.0%)	Presence: 1 (5.9%)	0.125	NS
Major biliary tract invasion	Presence: 0	Presence: 49 (41.2%)	Presence: 6 (35.3%)	0.065	NS
Surgical procedure	AR: 6 (75.0%) NAR: 2 (25.0%)	AR: 105 (88.2%) NAR: 14 (11.8%)	AR: 13 (76.5%) NAR: 4 (23.5%)	0.273	NS
Resection of extrahepatic bile duct	Presence: 1 (12.5%)	Presence: 34 (28.6%)	Presence: 1 (5.9%)	0.091	NS
Lymph node dissection	Presence: 5 (62.5%)	Presence: 106 (89.1%)	Presence: 15 (88.2%)	0.088	NS

HBsAg: hepatitis B surface antigen, HCV-Ab: hepatitis C virus antibody, AFP: alpha-fetoprotein, DCP: des-gamma-carboxy

prothrombin, CEA: carcinoembryonic antigen, CA19-9: carbohydrate antigen 19-9, AR: anatomical resection, NAR: non-anatomical resection, NS: not significant. **Bold font indicates statistical significance.**

Fig.1

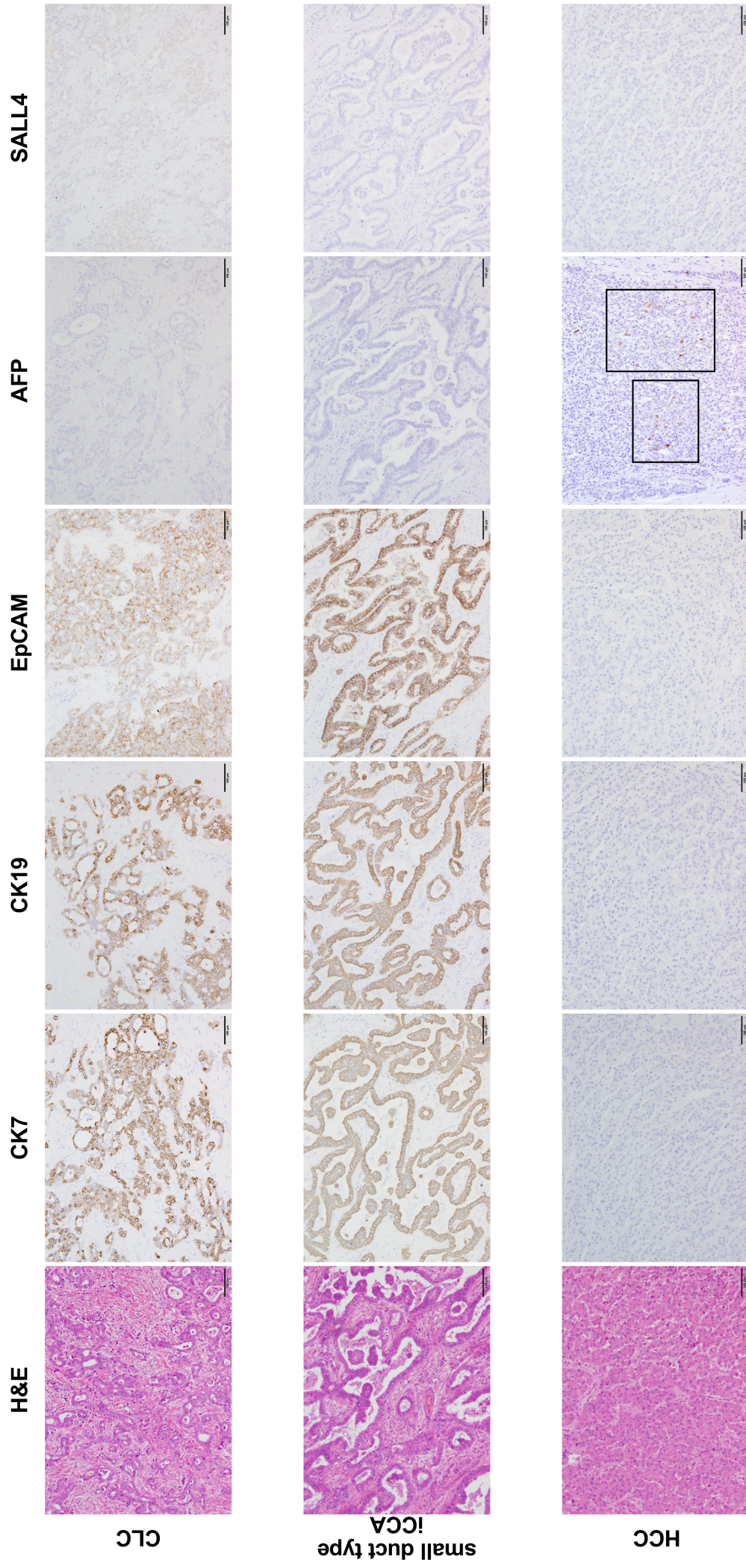


Fig.2

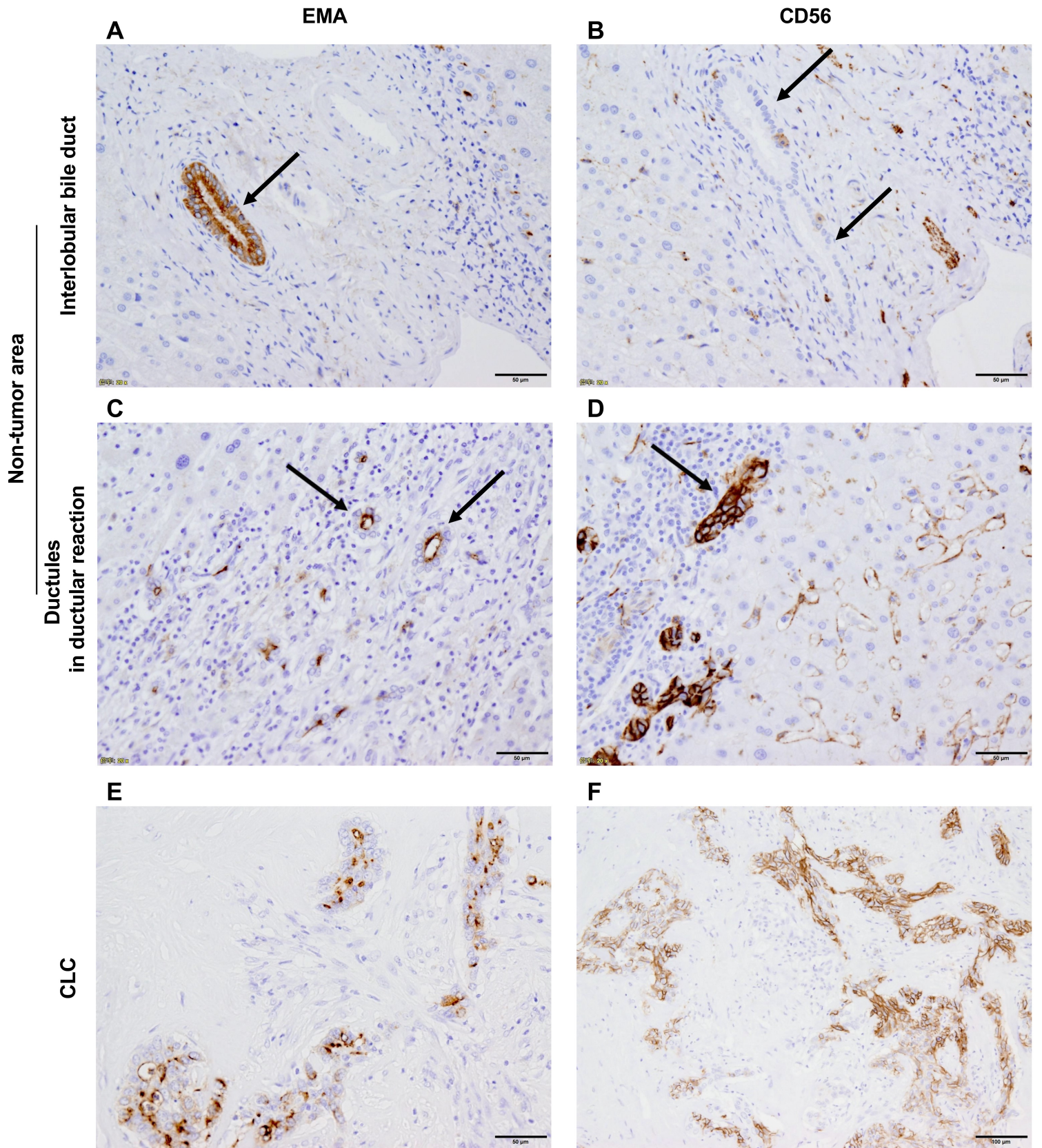


Fig.3

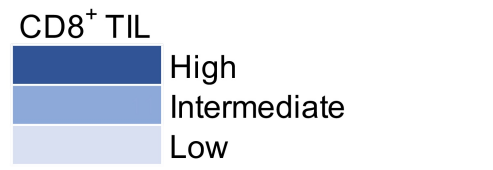
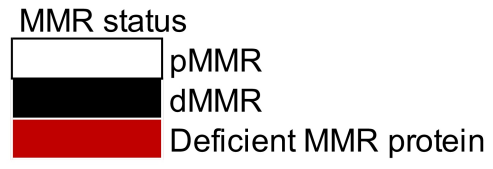
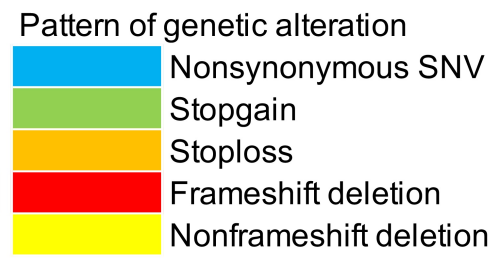
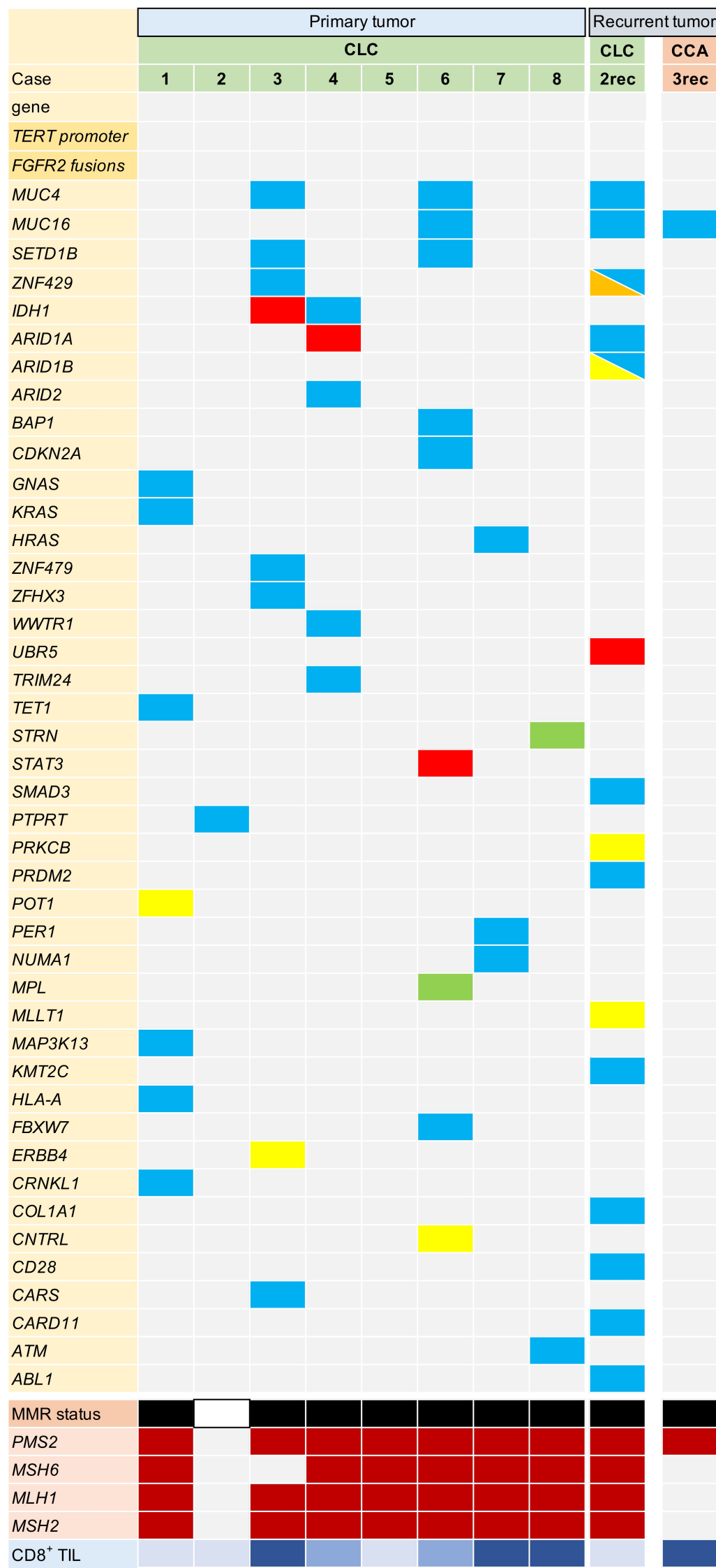


Fig.4

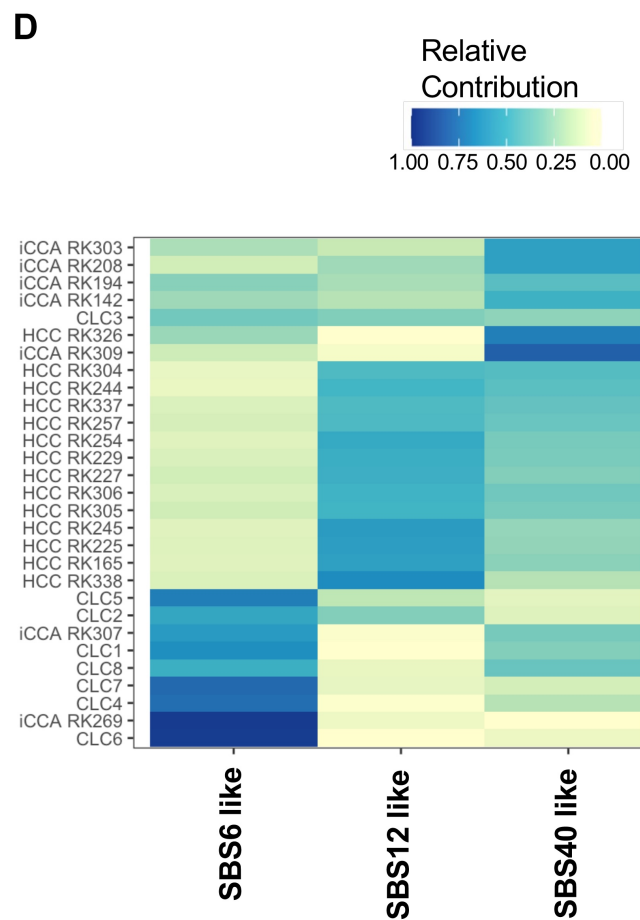
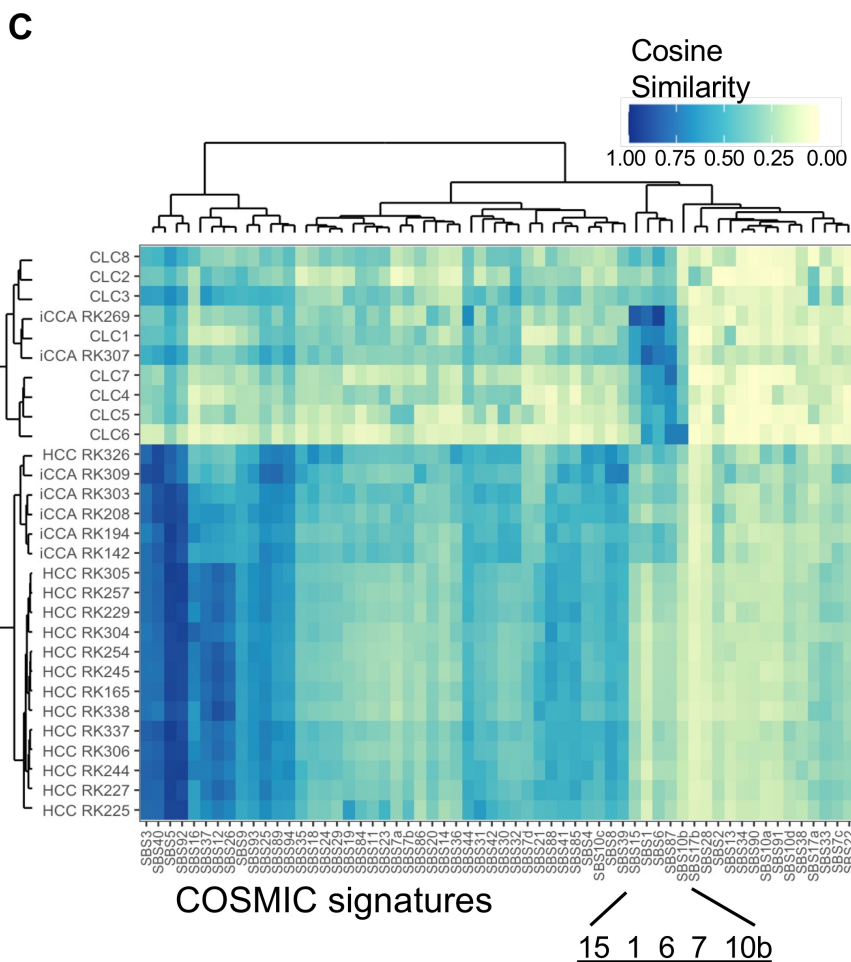
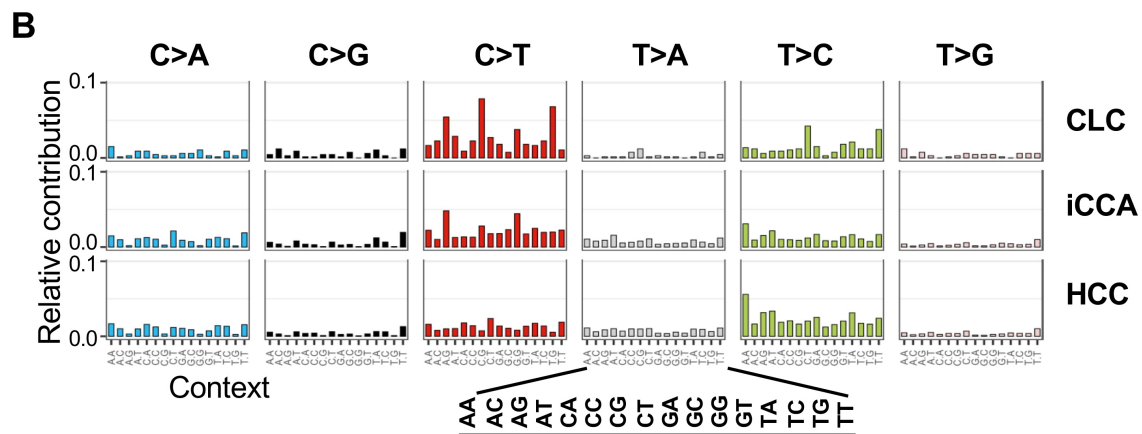
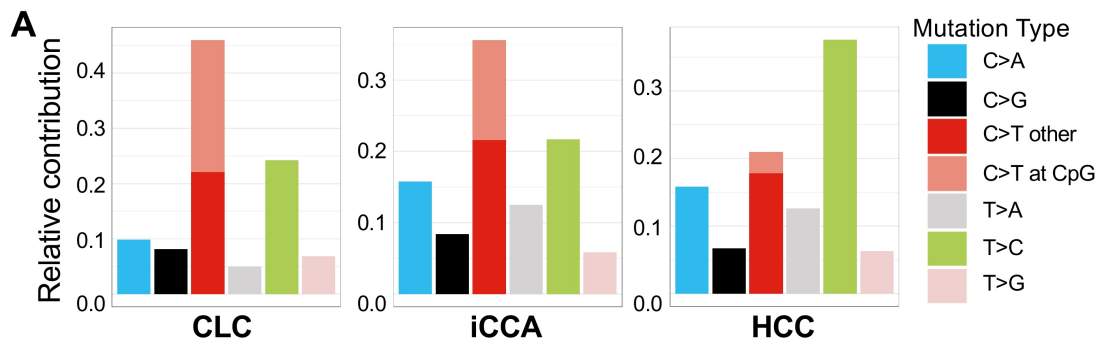
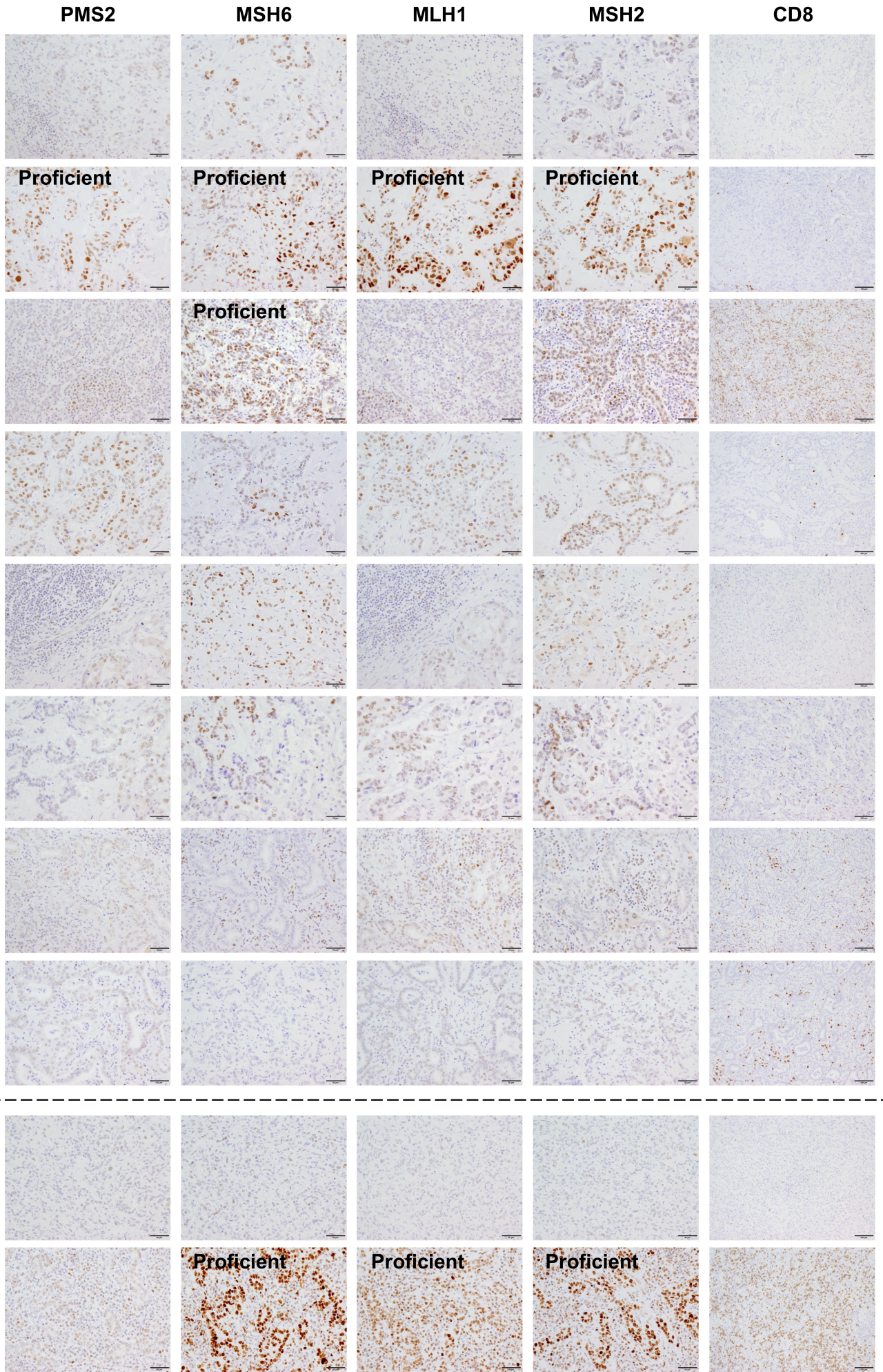


Fig. 5



Primary Tumor

Recurrent Tumor

Fig.6

